A systematic low-temperature neutron diffraction study of the $RBa_2Cu_3O_x$ (R=yttrium and rare earths; x=6 and 7) compounds

1994 J. Phys.: Condens. Matter 6 7963

(http://iopscience.iop.org/0953-8984/6/39/017)

J. Phys.: Condens. Matter 6 (1994) 7963–7976. Printed in the UK

A systematic low-temperature neutron diffraction study of the $RBa_2Cu_3O_x$ (R = yttrium and rare earths; $x = 6$ and 7) compounds

M Guillaume†, P Allenspach†, W Henggeler†, J Mesot†, B Roessli†, U Staub†, P Fischer†, A Furrer† and V Trounov‡

† Laboratorium für Neutronenstreuung, Eidgenönssische Technische Hochschule Zürich and Paul Scherrer Institut, CH-5232 Villigen PSI, Switzerland

‡ Petersburg Nuclear Physics Institute, Gatchina, St Petersburg 188350, Russia

Received 26 April 1994, in final form 5 July 1994

Abstract. The crystal structures of $RB2_2Cu_3O_x$ (R = Y and rare earths; $x = 6$ and 7) ceramic materials were investigated at 10 K by neutron diffraction and consistently analysed concerning systematic trends. Other than for non-superconducting $PrBa_2Cu_3O_7$ the lattice parameters and most interionic distances exhibit the well known lanthanide contraction behaviour, i.e., a linear relationship with the ionic radii of trivalent rare-earth ions. The only exceptions are associated with the apex oxygen O(1) ions: the chain copper Cu(1)–O(1) distances are constant within error limits, and the plane copper Cu(2)–O(1) distances are increasing across the rare-earth series. The much stronger increase of the distance Cu(2)–O(1) in the $RBa_2Cu_3O_6$ series compared to the $RBa_2Cu_3O_7$ series can be explained by the increase of T_c from 90 K for $YbBa_2Cu_3O_7$ to 96 K for $NbBa_2Cu_3O_7$. The smaller distance Cu(1)–O(1) for the $RBa_2Cu_3O_6$ series compared to the $RBa_2Cu_3O_7$ series may be related to the suggested double-well potential of the apical oxygen ion. For some interionic distances of $PrBa_2Cu_3O_7$ approximately parallel to the b direction (i.e., the chain direction) we determine by extrapolation a valence of +3.4 for the Pr ions. This indicates for $PrBa_2Cu_3O_7$ a highly anisotropic 4f-CuO_2 valence band hybridization. An important structural property with respect to the superconductivity is the puckering of the CuO_2 planes: the superconductivity is lost when the puckering angle exceeds a critical value of about 167.3°.

1. Introduction

The crystal structure, i.e., the arrangement of atoms in a material, largely determines its physical properties. Precise structure determination is then one of the basic requirements for any new substance. This is particularly true for the high-T_c perovskite-type compounds whose superconducting properties are strongly related to the structural details. In particular, one has to elucidate the oxygen coordination of the metal ions, e.g. the important features of the puckered copper–oxygen planes, various copper oxide bond lengths, etc. Neutron powder diffraction has repeatedly proven to be especially useful for such problems because of the great sensitivity for light atoms such as oxygen, compared to x-ray diffraction.

Apart from the anomalous non-superconducting $PrBa_2Cu_3O_7$ substitution of rare earths, R, for Y in $YBa_2Cu_3O_7$ is known to change superconductivity only slightly [1]: the superconducting transition temperature T_c gradually decreases from 96 K for R = Nd to 90 K for R = Yb. Our interest in the structural properties of these compounds has been motivated by neutron spectroscopic investigations of the crystal-field interaction at the R

0953-8984/94/397963+14$19.50

site which constitutes an ideal probe of the local symmetry and the charge distribution of the superconducting CuO_2 planes [2]. In order to be able to differentiate between the structure and charge aspects of the crystal-field interaction a consistent set of structural parameters was needed.

It is the purpose of the present work to provide for the first time such a consistent set of structural parameters at temperature $T = 10$ K for the entire series of compounds $RBa_2Cu_3O_x$ (R = Y, La, Pr, Nd, Sm, Eu, Gd, Dy, Ho, Er, Tm, Yb; $x \approx 6$ and 7). This was only possible due to the use of special isotopes (^{154}Sm, ^{153}Eu and ^{160}Gd) for the highly-neutron-absorbing rare-earth ions. Although there already exists in the literature a large number of neutron diffraction results for several compounds $RBa_2Cu_3O_x$ from thorough studies at many laboratories, a systematic analysis and intercomparison of all the existing structural data across the whole rare-earth series is made difficult by the lack of internal consistency, i.e., the existing structural information often exhibits considerable scattering due to differences in temperature, in the instrumental configuration of the neutron diffractometers, in sample preparation and characterization as well as in the methods of data treatment, which all give rise to systematic uncertainties. Recently Currie *et al* [3] studied the crystal structures of ceramic $RBa_2Cu_3O_7$ (R = Er, Ho, Dy) by high-resolution neutron diffraction at room temperature; however, the range of the lanthanide ionic sizes in this study is rather limited and general trends are more difficult to derive than our analyses which cover the whole rare-earth range. From the previous neutron diffraction investigations we should mention the basic work by Cava *et al* [4] on $YBa_2Cu_3O_x$ ($6 \leqslant x \leqslant 7$) in which the variation of particular copper–oxygen bond lengths with oxygen stoichiometry shows a similar dependence on oxygen concentration as the two-plateau superconducting transition temperature. In another work by Neumeier *et al* [5] on $Y_{1-y}Pr_yBa_2Cu_3O_7$ ($0 \leqslant y \leqslant 1$) interesting structural results have been obtained with respect to the valence state of Pr and the detrimental effect of Pr on T_c. The present low-temperature neutron diffraction investigation is an essential extension of our first structural study of $RBa_2Cu_3O_7$ compounds published in [6]. By a comparison of interatomic distances for both $RBa_2Cu_3O_6$ and $RBa_2Cu_3O_7$ across the whole rare-earth series, R, we shall prove anomalous structural properties of $PrBa_2Cu_3O_7$, such as valency deviating from 3+, and establish special puckering rules for superconducting CuO_2 planes. Moreover we can show clearly effects of lanthanide contraction and, on the other hand, invariance of the chain-copper–apex-oxygen distances.

2. Experimental procedures and results

Polycrystalline samples of $RBa_2Cu_3O_7$ were prepared by a careful standard sintering procedure as described in our previous paper [6] and by Rupp *et al* [7]. The compounds with R = La, Nd, Y, Ho, Er, Tm and Pr were prepared at our laboratory, whereas for R = Dy and Yb the sample preparation was performed at the Asea Brown Boveri Research Laboratory at Baden (Switzerland). Because of the high absorption cross section of thermal neutrons for R = Sm, Eu and Gd specimens were synthesized with the rare-earth isotopes ^{154}Sm, ^{153}Eu and ^{160}Gd, respectively, at the Petersburg Nuclear Physics Institute in Gatchina (Russia). In all cases fully oxygenated samples were prepared with an oxygen content close to $x = 7.0$, see table 1. The critical temperatures, T_c, were obtained from susceptibility measurements of the Meissner fraction. Examples are shown in figure 1. For the production of the oxygen-reduced compounds $x \approx 6$ we used the following procedure: under high-vacuum conditions (10^{-6} Torr) we heated our samples to 900 °C at a rate of 10 °C min^{-1}. After annealing for two hours at 900 °C, the released oxygen was pumped out, and then the

samples were cooled down to room temperature at a rate of 1 °C min^{-1}. Thus we obtained the oxygen content $x \approx 6.1$, see table 2.

The powder samples with a weight of about 20 g were filled into cylindrical vanadium containers of 12 mm diameter and 50 mm height under helium gas atmosphere and cooled to $T = 10$ K with use of a closed-cycle helium refrigerator. The neutron diffraction data were collected on the multidetector powder diffractometer DMC in high-resolution mode at the reactor SAPHIR in Würenlingen, Switzerland (liquid-nitrogen-cooled Si filter, vertically focusing Ge(311) monochromator, collimation $10'/-/ \geqslant 12'$, wavelength 1.6985(5) Å) [8]. The diffraction patterns (corrected for absorption according to the measured transmission) were refined employing the Rietveld method, using a modified program version by Wiles and Young [9] and neutron scattering lengths published by Sears [10]. A Gaussian peak shape was assumed, which generally holds well for DMC data [8].

The neutron diffraction patterns could be completely indexed on the basis of the well established model of an orthorhombic structure (figure 2(*a*)) for single-phase $RBa_2Cu_3O_7$ compounds corresponding to space group *Pmmm* and the tetragonal *P/4mmm* structure (figure 2(*b*)) for the $Rba_2Cu_3O_6$ compounds. Only in case of $LaBa_2Cu_3O_x$, $YbBa_2Cu_3O_x$ ($x = 6$ and 7) and $^{153}EuBa_2Cu_3O_6$ was there evidence of some minor impurity phases (about 3% and 2%, respectively) which could not be identified. This is the main reason for the poor fits in these cases (see tables 1 and 2). A total of 165 and 103 reflections were refined for orthorhombic $RBa_2Cu_3O_7$ and tetragonal $RBa_2Cu_3O_6$, respectively. Typical best fits for orthorhombic $TmBa_2Cu_3O_7$ and for tetragonal $TmBa_2Cu_3O_6$ are shown in figures 3(*a*) and 3(*b*), respectively. We only fitted the occupation numbers of the oxygen ions in the basal plane (O(4) and O(5)), whereas the others were fixed at their nominal values. Refined structural parameters and superconducting transition temperatures together with agreement factors are summarized in tables 1 and 2 for $RBa_2Cu_3O_7$ and $RBa_2Cu_3O_6$, respectively. Lattice parameters, unit cell volumes and relevant interatomic distances are plotted versus ionic radius in figures 4 to 12.

3. Discussion of results

The measured superconducting transition temperatures T_c of $RBa_2Cu_3O_7$ compounds (figure 1) confirm [1]. The lattice parameters *a*, *b* (figure 4) and *c* (figure 5) and the unit cell volume (figure 6) clearly show the expected lanthanide contraction behaviour, i.e., they exhibit a perfectly linear relationship when plotted versus the ionic radii for trivalent rare-earth ions [11], with two exceptions: firstly, for the $PrBa_2Cu_3O_7$ compound we infer a valence intermediate between +3 and +4 from the lattice parameter *c* and secondly the lattice parameters for $LaBa_2Cu_3O_7$ ($T_c = 50$, see figure 1(*a*)) do not follow the expected linear relationship. The details of this anomaly are discussed in a preliminary study of the $RBa_2Cu_3O_7$ compounds [6]. By reduction of the oxygen content in $LaBa_2Cu_3O_x$ from $x = 7$ to $x = 6$ the occupation of 12% Ba^{2+} ions at the La^{3+} site remains unchanged, but in contrast to $LaBa_2Cu_3O_7$ we do not observe any structural anomalies for $LaBa_2Cu_3O_6$ in the rare-earth series.

The slope of the lattice parameter *a* for the $RBa_2Cu_3O_7$ series is the same as for the $RBa_2Cu_3O_6$ series, indicating that there is no disorder in the basal plane along the *a* direction, implying negligible O(5) occupation. The slope of the lattice parameter *b* is slightly smaller than the slope of the lattice parameter *a* in the case of the $RBa_2Cu_3O_7$ compounds, according to the orthorhombicity shown in table 1. This could be due to the effect of minor oxygen vacancies in the Cu–O chains for the light rare earths which is

R		La	Pr	Nd	Sm	Eu	Gd	Dy	Y	Ho	Er	Tm	Yb
oxygen content x		7.06(5)	6.98(3)	6.98(3)	6.98(3)	6.98(3)	6.99(3)	6.98(3)	7.00(3)	7.02(3)	7.02(3)	7.02(3)	7.02(3)
T_c [K]		50(3)	0	96(1)	94(1)	95(1)	94(1)	92(1)	90(1)	90(1)	90(1)	90(1)	90(1)
radius for R^{3+} [Å]		1.160	1.126	1.109	1.079	1.066	1.053	1.027	1.019	1.015	1.004	0.994	0.985
R	B [Å^2]	0.1(1)	0.1(1)	0.1(1)	0.2(1)	0.1(1)	0.1(1)	0.1(1)	0.1(1)	0.2(1)	0.1(1)	0.1(1)	0.1(1)
Ba	B [Å^2]	0.2(1)	0.1(1)	0.1(1)	0.2(1)	0.1(1)	0.1(1)	0.1(1)	0.1(1)	0.2(1)	0.1(1)	0.1(1)	0.1(1)
	z	0.1779(6)	0.1803(5)	0.1809(4)	0.1819(4)	0.1822(5)	0.1826(4)	0.1830(5)	0.1834(4)	0.1832(3)	0.1848(4)	0.1835(3)	0.1847(4)
Cu(1)	B [Å^2]	1.2(1)	0.6(1)	0.7(1)	0.4(1)	0.4(1)	0.3(1)	0.3(1)	0.3(1)	0.3(1)	0.3(1)	0.3(1)	0.4(1)
Cu(2)	B [Å^2]	0.3(1)	0.4(1)	0.3(1)	0.2(1)	0.3(1)	0.3(1)	0.3(1)	0.2(1)	0.2(1)	0.3(1)	0.2(1)	0.3(1)
	z	0.3447(3)	0.3518(3)	0.3494(3)	0.3515(3)	0.3522(4)	0.3533(4)	0.3535(4)	0.3554(3)	0.3552(3)	0.3568(3)	0.3562(3)	0.3581(4)
O(1)	B [Å^2]	1.2(2)	0.7(1)	0.8(1)	0.5(1)	0.5(1)	0.5(1)	0.4(1)	0.4(1)	0.3(1)	0.5(1)	0.5(1)	0.5(1)
	z	0.1602(6)	0.1594(5)	0.1577(4)	0.1584(4)	0.1587(4)	0.1596(4)	0.1587(5)	0.1594(3)	0.1598(3)	0.1600(3)	0.1602(3)	0.1595(3)
O(2)	B [Å^2]	0.4(1)	0.6(1)	0.7(1)	0.4(1)	0.4(1)	0.4(1)	0.5(1)	0.4(1)	0.5(1)	0.6(1)	0.4(1)	0.5(1)
	z	0.3635(6)	0.3732(5)	0.3681(5)	0.3726(4)	0.3725(5)	0.3755(5)	0.3746(6)	0.3770(3)	0.3768(3)	0.3772(5)	0.3791(3)	0.3794(3)
O(3)	B [Å^2]	0.3(1)	0.6(1)	0.7(1)	0.4(1)	0.4(1)	0.4(1)	0.5(1)	0.4(1)	0.5(1)	0.6(1)	0.4(1)	0.5(1)
	z	0.3694(6)	0.3695(6)	0.3737(5)	0.3723(4)	0.3760(4)	0.3776(5)	0.3774(6)	0.3776(3)	0.3776(3)	0.3794(5)	0.3789(3)	0.3790(4)
O(4)	B [Å^2]	3.0(2)	1.5(3)	1.6(3)	2.1(2)	2.5(2)	2.0(2)	1.9(2)	1.7(2)	2.0(2)	1.6(2)	1.0(2)	1.5(2)
	n	0.76(2)	0.93(1)	0.93(1)	0.90(1)	0.92(1)	0.93(1)	0.92(1)	0.96(1)	0.96(1)	0.96(1)	0.99(1)	0.98(1)
O(5)	B [Å^2]	3.0(2)	1.5(3)	1.6(3)	2.1(2)	2.5(2)	2.0(2)	1.9(2)	1.7(2)	2.0(2)	1.6(2)	1.0(2)	1.5(2)
	n	0.30(3)	0.05(2)	0.05(2)	0.08(2)	0.06(2)	0.06(2)	0.06(2)	0.04(2)	0.06(2)	0.06(2)	0.03(2)	0.04(2)
a [Å]		3.903(1)	3.863(1)	3.856(1)	3.844(1)	3.836(1)	3.831(1)	3.820(1)	3.817(1)	3.815(1)	3.810(1)	3.805(1)	3.800(1)
b [Å]		3.920(1)	3.918(1)	3.912(1)	3.901(1)	3.897(1)	3.893(1)	3.885(1)	3.883(1)	3.882(1)	3.879(1)	3.876(1)	3.872(1)
c [Å]		11.735(1)	11.650(1)	11.719(1)	11.692(1)	11.682(1)	11.667(1)	11.646(1)	11.637(1)	11.635(1)	11.625(1)	11.616(1)	11.607(1)
(b - a) / (a+b) [%]		0.22	0.78	0.72	0.74	0.79	0.80	0.84	0.86	0.87	0.89	0.92	0.94
χ^2		11.73	4.50	4.32	10.70	16.13	15.23	11.6	6.12	7.53	8.34	3.70	7.69
R_I		4.90	3.96	4.51	5.11	5.62	4.89	5.80	3.62	6.83	3.04	3.34	6.78
R_{wp}		6.53	4.20	4.95	9.48	8.01	7.24	10.60	5.46	8.69	4.12	4.62	9.28
R_{exp}		2.91	2.13	2.85	3.52	1.98	2.01	4.20	2.84	2.36	1.43	2.40	1.54

Table 1. Structural parameters (and agreement values) of $RBa_2Cu_3O_7$ compounds (R = Y and rare earth) for $T = 10$ K, determined by neutron diffraction. The ionic radius for Pr^{4+} is 0.960 Å [11].

R		La	Pr	Nd	Sm	Eu	Gd	Dy	Y	Ho	Er	Tm	Yb
oxygen	content x	6.04(3)	6.15(3)	6.12(3)	6.11(3)	6.13(3)	6.06(3)	6.12(3)	6.11(3)	6.10(3)	6.08(3)	6.10(3)	6.14(3)
radius	for R^{3+} [Å]	1.160	1.126	1.109	1.079	1.066	1.053	1.027	1.019	1.015	1.004	0.994	0.985
R	B [Å^2]	0.1(1)	0.1(1)	0.1(1)	0.1(1)	0.1(1)	0.1(1)	0.1(1)	0.1(1)	0.1(1)	0.1(1)	0.1(1)	0.1(1)
Ba	B [Å^2]	0.2(1)	0.2(1)	0.2(1)	0.2(1)	0.2(1)	0.2(1)	0.2(1)	0.2(1)	0.2(1)	0.2(1)	0.2(1)	0.2(1)
	z	0.1908(4)	0.1910(4)	0.1908(4)	0.1912(4)	0.1906(4)	0.1930(4)	0.1945(4)	0.1935(4)	0.1943(3)	0.1946(4)	0.1949(3)	0.1950(4)
Cu(1)	B [Å^2]	0.3(1)	0.3(1)	0.3(1)	0.3(1)	0.3(1)	0.3(1)	0.3(1)	0.3(1)	0.4(1)	0.4(1)	0.3(1)	0.4(1)
Cu(2)	B [Å^2]	0.3(1)	0.3(1)	0.3(1)	0.3(1)	0.3(1)	0.3(1)	0.3(1)	0.3(1)	0.4(1)	0.4(1)	0.3(1)	0.4(1)
	z	0.3508(3)	0.3528(3)	0.3512(3)	0.3564(3)	0.3580(4)	0.3585(4)	0.3597(4)	0.3612(3)	0.3611(3)	0.3615(3)	0.3622(3)	0.3630(4)
O(1)	B [Å^2]	0.6(2)	0.7(2)	0.7(2)	0.6(2)	0.6(2)	0.5(2)	0.4(2)	0.4(2)	0.5(2)	0.4(2)	0.5(2)	0.5(2)
	z	0.1509(3)	0.1523(4)	0.1524(4)	0.1528(4)	0.1530(4)	0.1540(4)	0.1530(5)	0.1538(3)	0.1541(3)	0.1536(3)	0.1533(3)	0.1544(3)
O(2)	B [Å^2]	0.6(1)	0.7(1)	0.7(1)	0.6(1)	0.6(1)	0.5(1)	0.4(1)	0.4(1)	0.5(1)	0.4(1)	0.5(1)	0.5(1)
	z	0.3680(6)	0.3703(5)	0.3711(5)	0.3726(4)	0.3736(5)	0.3759(5)	0.3770(6)	0.3790(3)	0.3786(3)	0.3796(5)	0.3803(3)	0.3804(3)
O(3)	B [Å^2]	0.6(1)	0.7(1)	0.7(1)	0.6(1)	0.6(1)	0.5(1)	0.4(1)	0.4(1)	0.5(1)	0.4(1)	0.5(1)	0.5(1)
	z	0.3680(6)	0.3703(6)	0.3711(5)	0.3726(4)	0.3736(4)	0.3759(5)	0.3770(6)	0.3790(3)	0.3786(3)	0.3796(5)	0.3803(3)	0.3804(4)
O(4)	B [Å^2]	0.6(1)	0.7(1)	0.7(1)	0.6(1)	0.6(1)	0.5(1)	0.4(1)	0.4(1)	0.5(1)	0.4(1)	0.5(1)	0.5(1)
	n	0.04(3)	0.15(3)	0.12(3)	0.11(1)	0.13(3)	0.06(3)	0.12(3)	0.11(3)	0.10(3)	0.08(3)	0.10(3)	0.14(3)
a [Å]		3.915(1)	3.900(1)	3.893(1)	3.880(1)	3.879(1)	3.872(1)	3.860(1)	3.856(1)	3.855(1)	3.850(1)	3.843(1)	3.839(1)
b [Å]		3.915(1)	3.900(1)	3.893(1)	3.880(1)	3.879(1)	3.872(1)	3.860(1)	3.856(1)	3.855(1)	3.850(1)	3.843(1)	3.839(1)
c [Å]		11.850(1)	11.832(1)	11.830(1)	11.815(1)	11.811(1)	11.807(1)	11.796(1)	11.793(1)	11.792(1)	11.789(1)	11.785(1)	11.781(1)
χ^2		28.20	22.32	26.15	25.18	30.19	18.12	14.62	26.56	12.21	13.37	12.45	14.07
R_I		4.77	7.34	5.71	4.73	10.12	7.93	4.53	6.94	3.82	4.31	3.65	4.83
R_{wp}		16.25	14.31	13.27	12.55	13.52	11.97	9.15	15.22	8.69	8.99	9.54	11.77
R_{exp}		2.39	3.45	3.37	2.37	4.31	3.57	1.93	3.18	3.51	3.20	3.41	3.82

Table 2. Structural parameters (and agreement values) of $RBa_2Cu_3O_6$ compounds (R = Y and rare earth) for $T = 10$ K, determined by neutron diffraction.

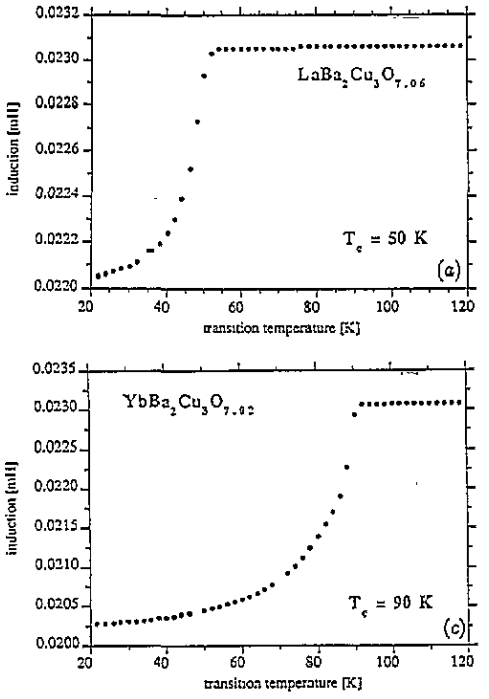

Figure 1. Temperature dependence of the magnetic susceptibility of (*a*) $LaBa_2Cu_3O_{7.06}$, indicating T_c = 50 K; (*b*) $NdBa_2Cu_3O_{6.98}$, indicating T_c = 96; (*c*) $YbBa_2Cu_3O_{7.02}$, indicating $T_c = 90$ K.

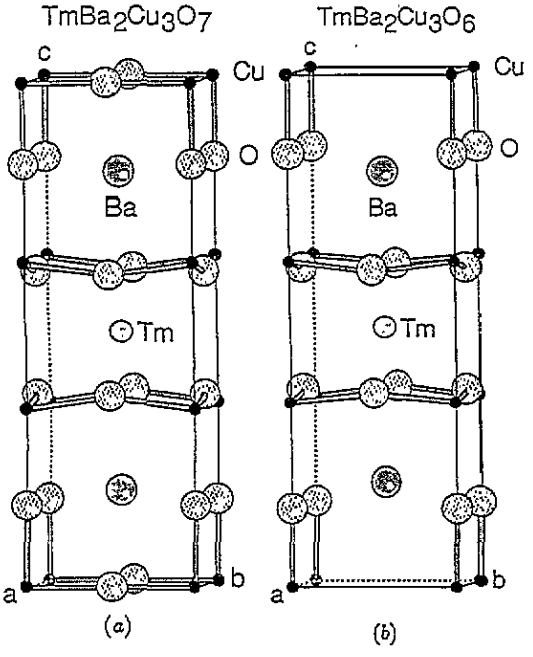

Figure 2. (*a*) Orthorhombic $TmBa_2Cu_3O_7$ structure; (*b*) tetragonal $TmBa_2Cu_3O_6$ structure.

demonstrated by a small reduction of the oxygen content from 7.02 for the Yb compound to 6.98 for the Nd compound. The slope of the lattice parameter c is much steeper in the $RBa_2Cu_3O_7$ series compared to the $RBa_2Cu_3O_7$ series. Such a change must be related with

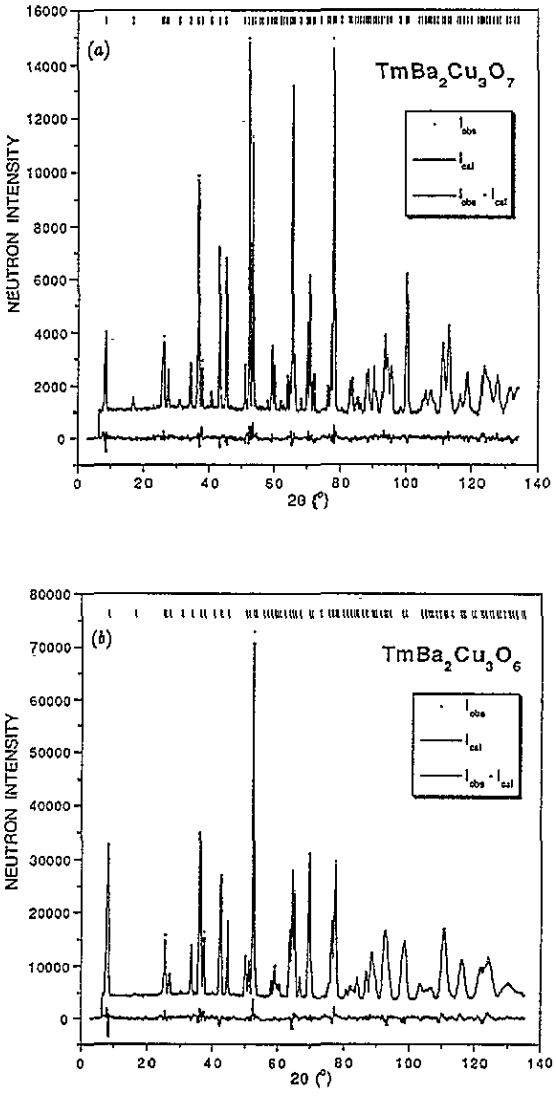

Figure 3. Observed, calculated and difference neutron diffraction patterns of (*a*) $TmBa_2Cu_3O_{7.02}$ at $T = 10$ K; (*b*) $TmBa_2Cu_3O_{6.11}$ at $T = 10$ K.

changes of the interionic distances along the *c* axis which will be discussed later in this paper. The slopes of the linear relationship of the unit cell volume are equal for both series. Even the $LaBa_2Cu_3O_7$ compound with reduced T_c caused by site mixing of La^{3+} ions and Ba^{2+} ions corresponds nicely to the linear dependence of the rare-earth contraction. The anomalous cell volume of $PrBa_2Cu_3O_7$ is most probably related to the intermediate-valence behaviour of the Pr ions.

We now proceed to discuss in detail some relevant interionic distances which generally are found to scale perfectly with the ionic radii for trivalent rare-earth ions as will be shown below. In all the subsequent figures this linear relationship is indicated by a straight line fitted to the data. The $LaBa_2Cu_3O_7$ and $PrBa_2Cu_3O_7$ compounds are excluded from this fit for reasons mentioned above.

Figure 7 shows the CuO_2 plane separations for the $RBa_2Cu_3O_7$ and $RBa_2Cu_3O_6$ compounds, i.e., the distances Cu(2)–Cu(2), which are particularly sensitive to the lanthanide

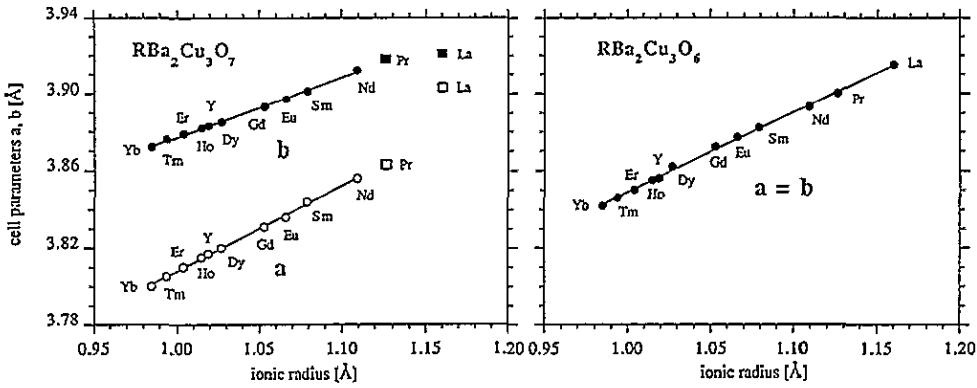

Figure 4. Lattice parameters a, b of $RBa_2Cu_3O_7$ and $RBa_2Cu_3O_6$ versus radius of trivalent R ions.

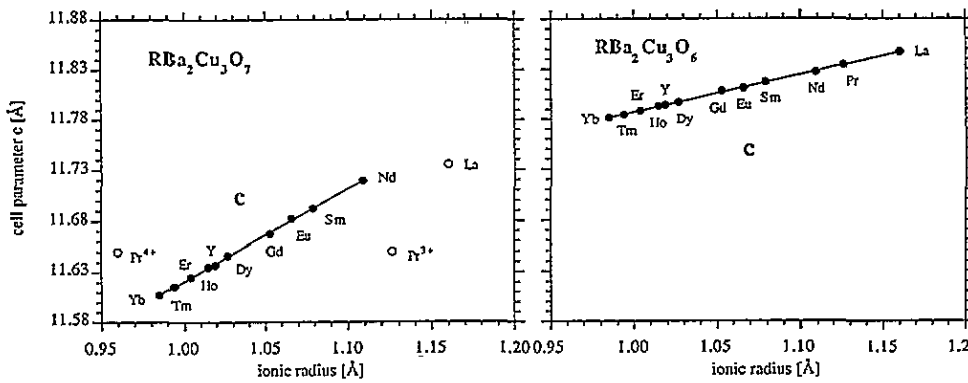

Figure 5. Lattice parameter c of $RBa_2Cu_3O_7$ and $RBa_2Cu_3O_6$ versus radius of trivalent R ions.

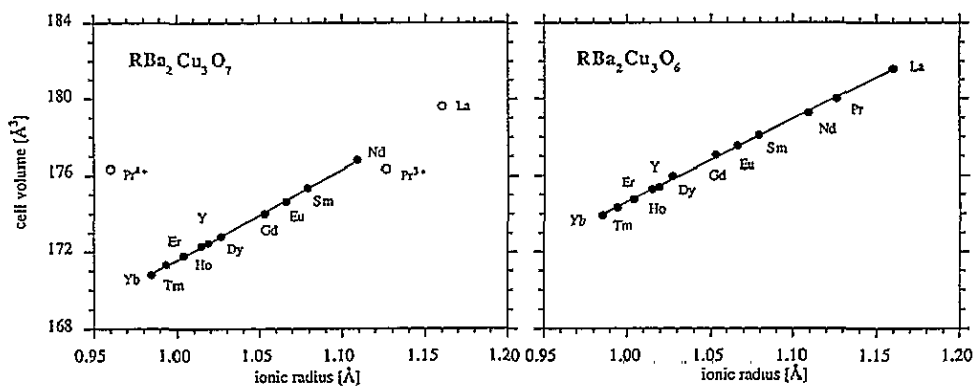

Figure 6. Unit cell volume $RBa_2Cu_3O_7$ and $RBa_2Cu_3O_6$ versus radius of trivalent R ions.

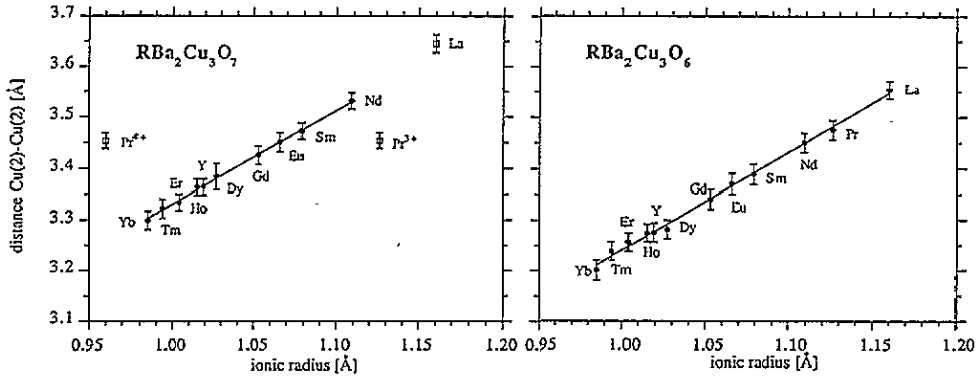

Figure 7. Distances Cu(2)–Cu(2) of $RBa_2Cu_3O_7$ and $RBa_2Cu_3O_6$ versus radius of trivalent R ions.

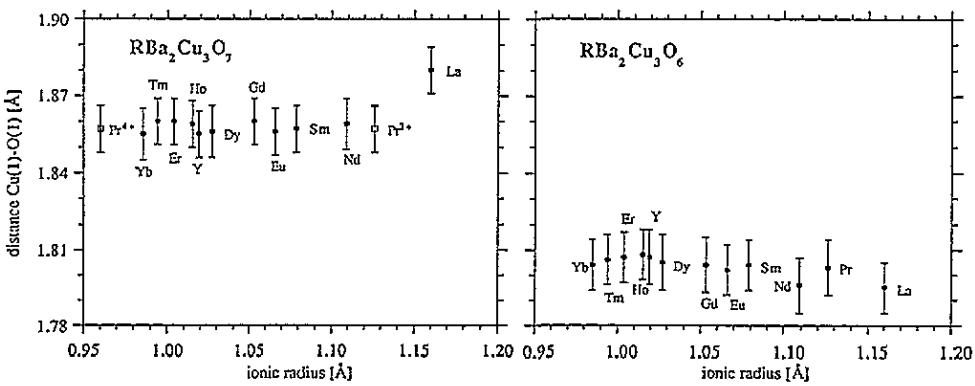

Figure 8. Distances Cu(1)–O(1) of $RBa_2Cu_3O_7$ and $RBa_2Cu_3O_6$ versus radius of trivalent R ions.

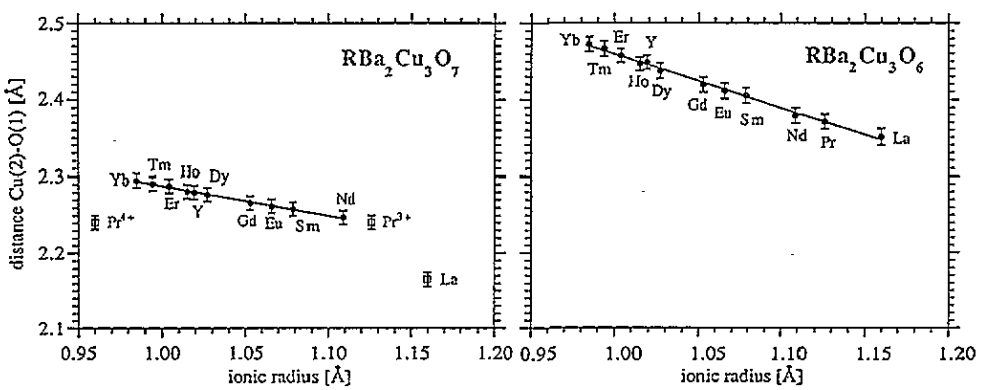

Figure 9. Distances Cu(2)–O(1) of $RBa_2Cu_3O_7$ and $RBa_2Cu_3O_6$ versus radius of trivalent R ions.

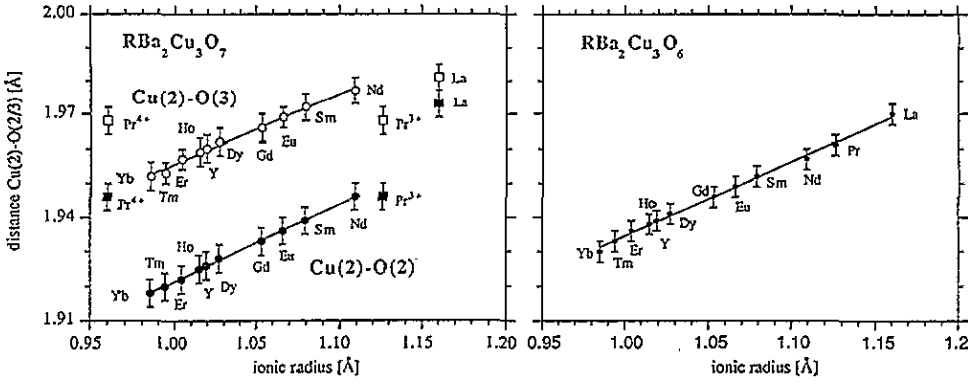

Figure 10. Distances Cu(2)–O(3) and Cu(2)–O(2) of $RBa_2Cu_3O_7$ and $RBa_2Cu_3O_6$ versus radius of trivalent R ions.

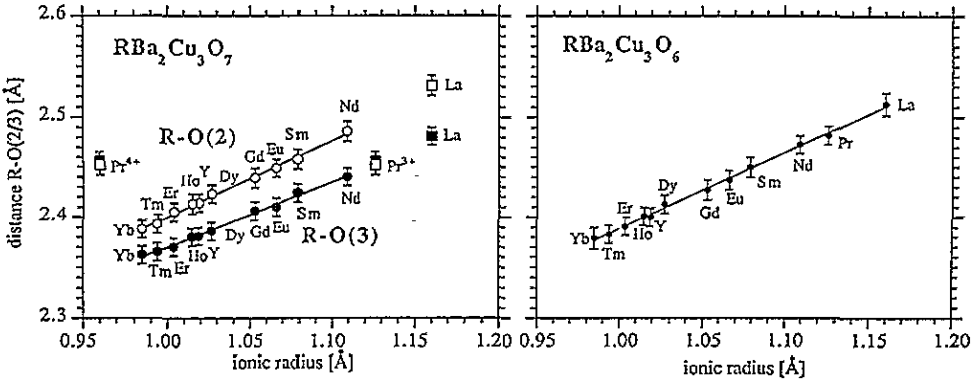

Figure 11. Distances R–O(2, 3) of $RBa_2Cu_3O_7$ and $RBa_2Cu_3O_6$ versus radius of trivalent R ions.

contraction, since the rare-earth ions are sandwiched between the CuO_2 planes. In fact, the Cu(2)–Cu(2) distances are found to contract twice as much as the lattice parameter c across the rare-earth series. For $PrBa_2Cu_3O_7$ we find an intermediate valence of +3.4 by interpolation. The Cu(2)–Cu(2) distances for both $PrBa_2Cu_3O_7$ and $PrBa_2Cu_3O_6$ are equal within error limits, whereas for all the other rare-earth compounds this distance is smaller by about 0.1 Å for $x = 6$ compared to $x = 7$. The plane copper Cu(2) spins are antiferromagnetically ordered below 370 K [12] for the non-superconducting $PrBa_2Cu_3O_7$ compound. This copper ordering persists for all oxygen contents in case of $PrBa_2Cu_3O_x$, whereas for the other rare-earth compounds long-range ordering of copper spins does not coexist with superconductivity. Even in the $RBa_2Cu_3O_x$ [4, 7] system the Cu(2)–Cu(2) distance remains constant in the non-superconducting range, where also the copper spins in the planes order antiferromagnetically. The constant Cu(2)–Cu(2) distance in the latter compounds indicates only small changes in the hybridization between the Pr ions and the ligand oxygen ions in the CuO_2 planes. This could also explain why the Néel temperatures of the antiferromagnetic Pr ordering in the $PrBa_2Cu_3O_x$ compounds are only slightly changed when going from $x = 7$ ($T_N = 17$ K) [13] to $x = 6$ ($T_N = 12$ K) [14].

The distance between the chain copper Cu(1) and the apex oxygen O(1) (figure 8) is constant for the whole rare-earth series for both $x = 6$ and $x = 7$ within error limits. The Cu(1)–O(1) distance has often been taken as a measure of the chain site copper valence; however, even for the anomalous Pr compound it remains constant. The distance Cu(1)–O(1) in the $RBa_2Cu_3O_6$ compounds is about 0.06 Å smaller than in the $RBa_2Cu_3O_7$ compounds. In the $RBa_2Cu_3O_6$ compounds, the valence at the copper chain site Cu(1) is reduced from 2^+ to 1^+. Assuming a double-minimum potential for the apex oxygen ions [15] we would therefore expect that in $RBa_2Cu_3O_7$ the O(1) ions preferentially occupy the upper part of the potential, whereas in $RBa_2Cu_3O_6$ the O(1) ions occupy the lower part of the potential. In this picture the change of the distance Cu(1)–O(1) of about 0.06 Å between $x = 7$ and $x = 6$ may be a characteristic value for the separation of the minima in the double-minimum potential. Salkola *et al* [16] observed a value of 0.09 Å for the splitting of the double-well potential, which is in good agreement with our result.

As shown in figure 9, the distance between the plane copper Cu(2) and the apical oxygen O(1) increases linearly in both $RBa_2Cu_3O_x$ series ($x = 6$ and $x = 7$) from the light to the heavy rare-earth compounds. Comparing the Cu(2)–O(1) distances of $RBa_2Cu_3O_6$ and $RBa_2Cu_3O_7$ compounds we observe a larger contraction for the heavier rare earths in the $RBa_2Cu_3O_7$ series, which also have slightly lower T_c values. T_c for $NdBa_2Cu_3O_7$ is 96 K (figure 1(*b*)) whereas $YbBa_2Cu_3O_7$ has $T_c = 90$ K (figure 1(*c*)). The observed higher T_c of the $NdBa_2Cu_3O_7$ compound may be related to the optimal doping regime, whereas the heavy rare earths are clearly in the overdoped regime and have a lower T_c [17]. As already discussed above, the slope for the distance Cu(2)–Cu(2) is equal for both oxygen concentrations $x = 6$ and $x = 7$ and also the Cu(1)–O(1) distance is constant in each series. Thus the different slope of the c axes in $RBa_2Cu_3O_7$ and $RBa_2Cu_3O_6$ is clearly related with the different slopes for the Cu(2)–O(1) distances. The shortening of the Cu(2)–O(1) bond across the rare-earth series, which is just the opposite compared to the lanthanide contraction, is much weaker in the oxygen $x = 7$ series as in the $x = 6$ series. This leads to a much steeper lanthanide contraction for the c axes in the oxygen $x = 7$ series than for the $x = 6$ series. This fact is once more an indication that the light rare earths are in the doped regime and have slightly higher T_c values than the heavier ones.

A comparison of the in-plane distances Cu(2)–O(2) and Cu(2)–O(3) for the $RBa_2Cu_3O_7$ compounds is shown in figure 10. While the bond length Cu(2)–O(2) is compatible with trivalent Pr ions, we derive an intermediate Pr valence of +3.4 from the distance Cu(2)–O(3), which is approximately oriented along the b chain direction. For the distances Cu(2)–O(2, 3) in the $RBa_2Cu_3O_6$ compounds (figure 10) we also observe the well known rare-earth contraction. The Cu(2)–O(2, 3) distance for the $RBa_2Cu_3O_6$ compounds is just the average of the Cu(2)–O(2) and Cu(2)–O(3) distances derived for $RBa_2Cu_3O_7$, which is clearly related to the change from the orthorhombic to the tetragonal structure.

Considering the distances between the rare earth and the plane oxygen ions we find slightly larger values for R–O(2) than for R–O(3) (figure 11) in the $RBa_2Cu_3O_7$ series whereas in the $RBa_2Cu_3O_6$ series the distances R–O(2, 3) are equal (figure 11) because of the tetragonal symmetry. The slope of the lanthanide contraction of R–O(2) in the $RBa_2Cu_3O_7$ series is equal to R–O(2, 3) in the $RBa_2Cu_3O_6$ series whereas it is slightly more shallow for the R–O(3) distances in the $RBa_2Cu_3O_7$. This indicates that the distance R–O(3) is becoming somewhat smaller when going from the heavy to the light rare earths. This could cause small hybridization effects between the rare-earth and the ligand oxygen atoms in the planes especially with the O(3). If we compare the linewidths of the crystalline-electric-field (CEF) splitting for R = Er [18], Nd [19] and Pr [20], we observe a broadening of these lines when going from Er to Nd; for Pr this effect is very strong. A calculation of

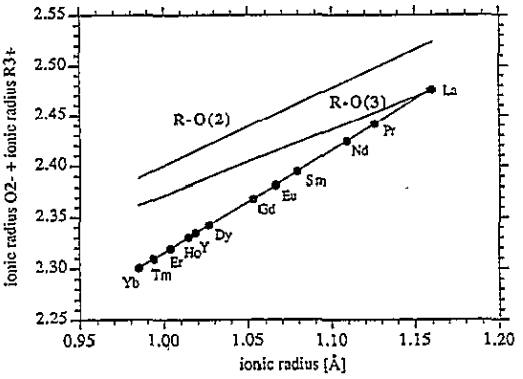

Figure 12. Model of hard sphere ions: sum of ionic radii of O^{2-} and R^{3+} [11] versus radius of trivalent R ions, in comparison to the distances R–O(2, 3) derived in the present work (see figure 11).

Goodman *et al* [21] also shows the tendency for hybridization for the light rare earths and motivated our explanation. Most interestingly, the distances R–O(3) in $RBa_2Cu_3O_7$ and R–O(2, 3) in $RBa_2Cu_3O_6$ are clearly compatible with Pr^{3+}, whereas from the distance R–O(2) we again derive a Pr valence of +3.4. Obviously, the hybridization between the Pr ion and the plane oxygen ions is exclusively associated with the O(2) ions, i.e., it acts mainly along the *b* chain direction and assumed oxygen holes are localized in CuO chains, and partially on Pr ions (in contrast to mobile oxygen holes in the CuO_2 planes in case of $YBa_2Cu_3O_7$). Takenaka *et al* [22] observed by polarized optical reflectivity of untwinned $PrBa_2Cu_3O_7$ crystals a large anisotropy of the optical conductivity in the *a*, *b* plane predominantly in the *b* direction. In $PrBa_2Cu_3O_7$ the two distances Pr–O(2) and Pr–O(3) are equal within the 2σ range, and they change much less when going from $x = 7$ to $x = 6$ compared to the other $RBa_2Cu_3O_x$ compounds which suggests that the change in hybridization of the Pr ions must be rather small. Booth *et al* [23] determined from x-ray absorption fine structure a Pr–O bond length of about 2.45 Å, which is in good agreement with our result, but they could not distinguish between the *a* and *b* directions. In this context, a simple hard-sphere model turns out to be very illustrative. In figure 12 we plot the sum of the ionic radii of O^{2-} and R^{3+} versus the rare-earth radii and compare our calculation with the R–O(2) and R–O(3) distances derived in the present work. The sum of the two ionic ions is very close to the Pr–O(3) distance which may indicate an electronic change in the $PrBa_2Cu_3O_7$ compound. There may be a hybridization with the O(3) oxygen atom. This hybridization between the $2p_z$ and the 4f electrons may strongly affect the Pr–O(2) bond by a redistribution of the charge. This electronic change is clearly supported by the shortening of the Cu(2)–O(3) bond which indicates that the correlation between the copper Cu(2) and the oxygen O(2, 3) changes a great deal, which could cause the loss of superconductivity.

A final comment concerns the puckering of the CuO_2 planes. The angles Cu(2)–O(2)–Cu(2) (figure 13) are constant in the $RBa_2Cu_3O_7$ series with a value of $164.5° \pm 0.4°$, with the exception of the $PrBa_2Cu_3O_7$ and the $LaBa_2Cu_3O_7$ compounds whereas the Cu(2)–O(3)–Cu(2) angles (figure 13) are decreasing for the smaller to the larger rare-earth ions in the $RBa_2Cu_3O_7$ series. This fact can be explained by the change of the orthorhombicity, which is related to a weaker increase of the *b* axis across the rare-earth series compared to the *a* axis. If we assume the same slope for the *a* and *b* axes and take those values to calculate the Cu(2)–O(3)–Cu(2) angles, we get for all rare earths the same angle of about $165.5° \pm 0.4°$. The $PrBa_2Cu_3O_7$ compound clearly does not follow this linear behaviour, the Cu(2)–O(3)–Cu(2) angle (figure 13) is much larger, having a value of $168° \pm 0.4°$. The angles Cu(2)–O(2, 3)–Cu(2) (figure 13) of the $RBa_2Cu_3O_6$ series are constant with a value of $168° \pm 0.4°$ across the rare-earth series with the exception of

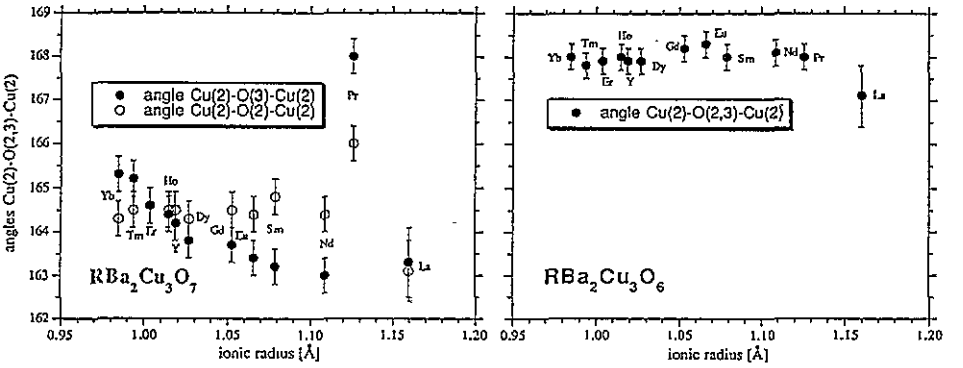

Figure 13. Angles Cu(2)–O(2, 3)–Cu(2) of $RBa_2Cu_3O_7$ and $RBa_2Cu_3O_6$ versus radius of trivalent R ions.

the $LaBa_2Cu_3O_6$ compound. The anomalous angles observed for $LaBa_2Cu_3O_x$ for $x = 6$ and $x = 7$ are presumably related to the site mixing of La^{3+} and Ba^{2+}. The observed angle Cu(2)–O(3)–Cu(2) for the $PrBa_2Cu_3O_7$ compound (which is equal to the angles of non-superconducting $RBa_2Cu_3O_6$ compounds) clearly gives evidence for the loss of the superconductivity. That loss of superconductivity is obviously related to a stretching of the puckering angle which is also observed in the $ErBa_2Cu_3O_x$, $NdBa_2Cu_3O_x$, $HoBa_2Cu_3O_x$ and $TmBa_2Cu_3O_x$ ($6 \leqslant x \leqslant 7$) systems; there, the deoxygenation process raises its value, and the transition to the semiconducting phase occurs above a critical angle of 167.2° [7]. Recently, Büchner *et al* [24] also observed a critical angle for the buckling for the disappearance of the superconductivity in rare-earth-doped $La_{1-x}Sr_xCuO_4$.

4. Conclusions

We provide for the first time a consistent set of structural data for carefully prepared $RBa_2Cu_3O_x$ ($x = 6$ and 7) compounds at $T = 10$ K and analysed the results with respect to systematic trends. The lattice parameters and a large number of interionic distances are found to scale linearly with the ionic radii of trivalent rare-earth ions according to the well known lanthanide contraction whose effect is therefore predominantly a purely geometrical one due to the expansion of the lattice with increasing size of the R ion when going from Yb to La. We also observe a change of the puckering of the CuO_2 planes between $x = 7$ and $x = 6$ which is clearly related to the loss of superconductivity when the puckering angle exceeds a critical value of about 167.3°. By interpolation we find that the Pr ions in $PrBa_2Cu_3O_7$ associated with the interionic distances along the b direction have an intermediate valence of +3.4, which is comparable to the value of +3.3 derived by Neumeier *et al* [5] from $Y_{1-y}Pr_yBa_2Cu_3O_7$ structural data. This higher valence observed for the $PrBa_2Cu_3O_7$ compound may be explained in terms of electronic changes in the CuO_2 planes which yields an anisotropic Pr(4f)–CuO_2 valence band hybridization occurring predominantly along the b chain direction. Recently published reflection electron energy-loss (EELS) and near-edge extended x-ray absorption fine-structure spectroscopy (NEXAFS) measurements [25] on single crystals $Y_{1-y}Pr_yBa_2Cu_3O_7$ ($y = 0$, 0.5, 1) also indicate very strong hybridization of O(2p)–Pr(4f) orbitals. The small changes in the interionic distances Pr–O(2, 3) and Cu(2)–Cu(2) when going from $PrBa_2Cu_3O_7$ to $PrBa_2Cu_3O_6$, indicate only

minor changes in Pr–oxygen hybridization. The strong hybridization of the Pr–O(2) bond along the *b*-axis may be the reason for the unusually high Néel temperatures associated with the Pr sublattice of about 17 K [13] for $PrBa_2Cu_3O_7$ and 12 K [14] for $PrBa_2Cu_3O_6$, which exceed the values of T_N observed for the other $RBa_2Cu_3O_x$ compounds by roughly an order of magnitude. The hybridization leads to partial delocalization of the 4f electrons which manifests itself in drastically enhanced linewidths of crystal-field transitions as observed in neutron spectroscopic investigations of $PrBa_2Cu_3O_x$ ($x = 6$ and 7) [20, 26, 27].

Acknowledgments

We would like to thank Professor P. Brüesch *et al*, Asea Brown Boveri Research Laboratory, Baden (Switzerland) for initial help in the preparation of some samples. Financial support by the Swiss National Science Foundation and the Russian National Program for High-Temperature Superconductors is gratefully acknowledged.

References

[1] Tarascon J M, McKinnon W R, Greene L H, Hull G W and Vogel E M 1987 *Phys. Rev.* B **36** 226
[2] Furrer A, Allenspach P, Mesot J, Staub U, Blank H, Mutka H, Vettier C, Kaldis E, Karpinski J, Rusiecki S and Mirmelstein A 1991 *Eur. J. Solid State Inorg. Chem.* **28** 627
[3] Currie D B and Weller M T 1993 *Physica* C **214** 204
[4] Cava R J, Hewat A W, Hewat E A, Batlogg B, Marezio M, Rabe K M, Krajewski J J, Peck W F and Rupp L W 1990 *Physica* C **165** 419
[5] Neumeier J J, Bjornholm T, Maple M B, Rhyne J J and Gotaas J A 1990 *Physica* C **166** 191
[6] Guillaume M, Allenspach P, Mesot J, Roessli B, Staub U, Fischer P and Furrer A 1993 *Z. Phys.* B **90** 13
[7] Rupp B, Pörschke E, Meuffels P, Allenspach P and Fischer P 1989 *Phys. Rev.* B **40** 4472
[8] Schefer J, Fischer P, Heer H, Isacson A, Koch M and Thut R 1990 *Nucl. Instrum. Methods* A **288** 477
[9] Wiles D B and Young R A 1981 *J. Appl. Crystallogr.* **14** 149
[10] Sears V F 1992 *Neutron News* **23** 26
[11] Shannon R D 1976 *Acta Crystallogr.* A **32** 751
[12] Rosov N, Lynn J W, Cao G, O'Reilly J W, Pernambuco-Wise P and Crow J F 1994 *Phys. Rev.* B submitted
[13] Li W-H, Lynn J W, Skanthakumar S, Clinton T W, Kebede A, Jee C-S, Crow J E and Mihalisin T 1989 *Phys. Rev.* B **40** 5300
[14] Guillaume M, Fischer P, Roessli B, Podlesnyak A, Schefer J and Furrer A 1993 *Solid State Commun.* **88** 57
[15] Bishop A R, Martin R L, Müller K A and Tesanovic Z 1989 *Z. Phys.* B **76** 17
[16] Salkola M I, Bishop A R, Mustre de Leon J and Trugman S A 1994 *Phys. Rev.* B **49** 3671
[17] Lütgemeier H, Heinmaa I, Wagener D and Hosseini S M 1993 *Proc. Workshop on Phase Separation in Cuprate Superconductors (Cottbus, Germany)*
[18] Mesot J, Allenspach P, Staub U, Furrer A, Mutka H, Osborne R and Taylor A 1993 *Phys. Rev.* B **47** 6027
[19] Allenspach P, Mesot J, Staub U, Guillaume M, Furrer A, Yoo S-I, Kramer J, McCallum R W, Malletta H, Blank H, Mutka H, Osborn R, Arai M, Bowden Z and Taylor A D 1994 *Z. Phys.* at press
[20] Jostarndt H-D, Walter U, Harnischmacher J, Kalenborn J A, Severing A and Holland-Moritz E 1992 *Phys. Rev.* B **46** 14872
[21] Goodman G L and Soderholm L 1990 *Physica* C **171** 528
[22] Takenaka K, Imanaka Y, Tamasaku K, Ito T and Uchida S 1992 *Phys. Rev.* B **45** 5833
[23] Booth C H, Bridges F, Boyce J B, Claeson T, Zhao Z X and Cervantes P 1994 *Phys. Rev.* B **49** 3432
[24] Büchner B, Breuer M, Freimuth A and Kampf A P 1994 *Phys. Rev. Lett.* submitted
[25] Hartmann A, Russell G J, Frentrup W and Taylor K N R 1994 *Solid State Commun.* **89** 77
[26] Soderholm L, Loong C K, Goodman G L and Dabrowski B D 1991 *Phys. Rev.* B **43** 7923
[27] Boothroyd A T, Doyle S M and Osborn R 1993 *Physica* C **217** 425